

15-5-2008

Analytical and numerical modeling of consolidation by vertical drain beneath a circular embankment

Buddhima Indraratna
University of Wollongong, indra@uow.edu.au

Ala N. Aljorany
ala@uow.edu.au

Cholachat Rujikiatkamjorn
University of Wollongong, cholacha@uow.edu.au

Follow this and additional works at: <https://ro.uow.edu.au/engpapers>



Part of the [Engineering Commons](#)

<https://ro.uow.edu.au/engpapers/450>

Recommended Citation

Indraratna, Buddhima; Aljorany, Ala N.; and Rujikiatkamjorn, Cholachat: Analytical and numerical modeling of consolidation by vertical drain beneath a circular embankment 2008.
<https://ro.uow.edu.au/engpapers/450>

**ANALYTICAL AND NUMERICAL MODELLING OF CONSOLIDATION BY SAND
DRAINS BENEATH A CIRCULAR EMBANKMENT**

Buddhima Indraratna

BSc (Hons., Lond.), MSc (Lond.), DIC, PhD (Alberta), FIEAust., FASCE, FGS

Professor of Civil Engineering, Faculty of Engineering,

University of Wollongong, Wollongong City, NSW 2522, Australia.

Ala Aljorany

BSc.(CE), MSc.(CE), PhD.(SM)

Asst. Professor, Dept. of Civil Eng, University of Baghdad, IRAQ

Endeavour Research Fellow (DEST), Civil Engineering Division, Faculty of Engineering,

University of Wollongong, Wollongong City, NSW 2522, Australia

Cholachat Rujikiatkamjorn

BEng (Hons), MEng (AIT), PhD

Research Associate, Civil Engineering Division, Faculty of Engineering,

University of Wollongong, Wollongong City, NSW 2522, Australia

Submitted to: THE INTERNATIONAL JOURNAL OF GEOMECHANICS

GM/2007/000357

Author for correspondence:

Prof. B. Indraratna

Faculty of Engineering

University of Wollongong

Wollongong, NSW 2522

Australia.

Ph: +61 2 4221 3046

Fax: +61 2 4221 3238

Email: indra@uow.edu.au

ANALYTICAL AND NUMERICAL MODELLING OF CONSOLIDATION BY VERTICAL DRAIN BENEATH A CIRCULAR EMBANKMENT

Buddhima Indraratna, Ala Aljorany and Cholachat Rujikiatkamjorn

Abstract: In the analysis of axisymmetric problems, it is often imperative that aspects of geometry, material properties and loading characteristics are either maintained as constants or represented by continuous functions in the circumferential direction. In the case of radial consolidation beneath a circular embankment by vertical drains (i.e. circular oil tanks or silos), the discrete system of vertical drains can be substituted by continuous concentric rings of equivalent drain walls. An equivalent value for the coefficient of permeability of the soil is obtained by matching the degree of consolidation of a unit cell model. A rigorous solution to the continuity equation of radial drainage towards cylindrical drain walls is presented and verified by comparing its results with existing unit cell model.

The proposed model is then adopted to analyse the consolidation process by vertical drains at the Skå-Edeby circular test embankment (Area II). The calculated values of settlement, lateral displacement and excess pore water pressure indicate good agreement with the field measurements.

Key words: finite element analysis, soil consolidation, soil stabilisation, subsurface drainage.

INTRODUCTION

Installation of vertical drains is one of the most widely used techniques for improving the engineering characteristics of soft clays. The main function of vertical drain application is to accelerate soil consolidation by shortening the drainage path and activating radial drainage, thereby increasing the shear strength of the soil while reducing its post-construction settlement (Holtz et al., 1991). The dissipation of excess pore water pressure occurs faster in the radial direction due to the greater coefficient of soil permeability in the horizontal direction and the reduced drainage path. The consolidation time can be reduced to achieve a required degree of consolidation by selecting a suitable drain spacing and an appropriate installation pattern (Jamiolkowski et al., 1983).

The theoretical solution of radial drainage consolidation was first proposed by Barron (1948) based on a unit cell (i.e. single drain surrounding by a soil cylinder). Further studies on the unit cell consolidation were conducted by Yoshikumi and Nakanodo (1979) and Hansbo (1981) which lead to the following well-known equation:

$$[1] \quad U_h = 1 - \exp\left(-\frac{8T_h}{\mu}\right),$$

In the above equation,

$$[1a] \quad T_h = \frac{c_h \cdot t}{d_e^2}$$

$$[1b] \quad \mu = \ln\left(\frac{n}{s}\right) + \left(\frac{k_h}{k_s}\right) \ln(s) - 0.75 + \pi(2lz - z^2) \left(\frac{k_h}{q_w}\right)$$

$$[1c] \quad n = (d_e/d_w)$$

$$[1d] \quad s = (d_s/d_w),$$

where,

U_h = average degree of lateral consolidation, T_h = time factor, c_h = coefficient of consolidation in radial direction, t = time, d_e = diameter of soil cylinder, μ = factor accounting for smear and well resistance. d_w = equivalent diameter of the drain, d_s = diameter of smear zone, l = drain length, q_w = discharge capacity of the drain, z = depth of horizontal plane under consideration, k_h and k_s = coefficients of horizontal permeability in the smear zone and undisturbed zone, respectively.

The unit cell analysis is accurate when applied at the embankment centreline where the lateral displacements are zero. In practice, the subsoil in which hundreds of drains are installed is usually not uniform, and the process of consolidation is not always a one dimensional problem (Indraratna et al., 1992). The numerical techniques including the finite element method (FEM) are essential for the analysis and design of multi-drain systems, apart from the effect of variability in soil properties at a site (Hird et al., 1992, Indraratna and Redana 2000, Chai et al. 2001). Various studies including Olson (1998) have indicated that conducting a finite element analysis for multi-drains is often time-consuming, and that it is related to the convergence of solution that inevitably requires large computer memory and a large number of iterations. However, the complexity of the multi-drains (3D) problem can be reduced to an equivalent two-dimensional (2D) situation by transforming the in-situ (3D) soil parameters into equivalent 2D parameters or making other simplifications. For example, Hird et al. (1992) employed a one dimensional drainage element to simulate a vertical drain. Chai et al. (2001) presented a simple approximation method by which the unit cell can be modelled as a soil with an equivalent vertical permeability. Indraratna and Redana (2000) presented a plane strain (2D) model that takes into account the effect of smear and well resistance.

It can be noted that most of the previous studies have been devoted to model multi-drain systems for embankment strip loading (plane strain). So far, no study has been conducted to model soil consolidation via vertical drains beneath a circular loaded area, where the system conforms to an axisymmetric problem.

In this study, the consolidation process accelerated by vertical drains below a circular embankment is analysed using the finite element method. An equivalent axisymmetric solution for concentric rings of vertical drains is obtained and validated using a numerical scheme and its results with Hansbo (1997) unit cell model. The FEM code ABAQUS is then used to analyse the performance of a full-scale test embankment constructed at Skå-Edeby, Stockholm-Arlanda Airport. The numerical predictions are compared with the available field data.

MATHEMATICAL FORMULATION

Vertical drains are generally installed either as an equilateral triangular, square or circular arc pattern. The circular arc installation pattern with each arc at the design spacing can be used with a large crane. It is noted that the square pattern can be easily controlled in the field, although the triangular pattern gives more uniform settlement than the square one (Rixner et al., 1986). Figure 1 shows a plan view and vertical cross section of a typical vertical drain installation pattern including some field instrumentation beneath a circular embankment at Ska-Edeby (Hansbo 1960) While the consolidation of soil around an individual vertical drain can be readily analysed as a single unit cell, in order to analyse a multi-drain system under an axisymmetric condition, one must determine the equivalent soil parameters that give the same time- settlement response in the field. In such a transformation, each drain element should behave as a part of concentric cylindrical drain wall with an increasing perimeter with

the radial distance from the centreline (Fig. 2). Figure 3 shows a concept of cylindrical soil-drain wall.

The main assumptions made in the authors' analysis are summarised below:

- Equal strain assumption (small strain) and Darcy's Law are valid.
- Only vertical strains are allowed.
- The soil is fully saturated, and the permeability of the soil is assumed to be constant during consolidation.
- Well resistance is neglected due to the sufficient discharge capacity of the drain, thereby the pore pressure at the drain interface is assumed to be zero.
- Each set of vertical drains located at the same radial distance from the line of axisymmetric is modelled as a continuous cylindrical drain wall of radius ($r_i = i.S$) where S is the spacing of the drains and i is the number of that set ($i = 1, 2, 3...$) as shown in Figure 3. For ($i > 1$), each cylindrical drain wall lies in the middle of a revolving prism of soil which has a thickness of S .
- It is assumed that the cylindrical drain wall has a negligible thickness.
- Across the inner and outer boundary of each revolving prism of soil (Fig. 3), no flow is allowed, and for relatively long vertical drains, only radial (horizontal) flow is permitted.

Development of Mathematical Formulation

Considering the inner hollow cylindrical soil wall ($r_i - S/2 \leq r \leq r_i$), the flow rate in the radial direction from the inner impermeable boundary to the hollow cylindrical drain wall is expressed by Darcy's law:

$$[2] \quad \frac{\partial Q}{\partial t} = \frac{k_h}{\gamma_w} \frac{\partial u}{\partial r} A$$

where, Q is the flow in the soil mass, u is the excess pore pressure due to preloading, A is the cross sectional area of the flow at distance r that is equal to $2\pi r(dz)$.

The rate of volume change in the vertical direction of the soil mass is expressed by:

$$[3] \quad \frac{\partial V}{\partial t} = \frac{\partial \varepsilon}{\partial t} \pi \left((r_i - S/2)^2 - r^2 \right) dz$$

where, V is the volume of the soil mass, and ε is the vertical strain.

The radial flow rate is assumed to be equal to the rate of volume change of the soil mass in the vertical direction, therefore,

$$[4] \quad \frac{k_h}{\gamma_w} \frac{\partial u}{\partial r} 2\pi r(dz) = \frac{\partial \varepsilon}{\partial t} \pi \left((r_i - S/2)^2 - r^2 \right) dz$$

The excess pore pressure gradient can be derived by rearranging Equation (4) as:

$$[5] \quad \frac{\partial u}{\partial r} = \frac{\gamma_w}{2k_h} \frac{\partial \varepsilon}{\partial t} \frac{\left((r_i - S/2)^2 - r^2 \right)}{r} \quad \text{for } r_i - S/2 \leq r \leq r_i$$

Integrating Equation (5) in the radial direction with the boundary condition ($u=0$ at $r=r_i$), the distribution of excess pore pressure u in Zone A ($r_i - S/2 \leq r \leq r_i$) can be expressed by:

$$[6] \quad u_A = \frac{\gamma_w}{2k_h} \frac{\partial \varepsilon}{\partial t} \left((r_i - S/2)^2 \ln \left(\frac{r}{r_i} \right) - \frac{1}{2} (r^2 - r_i^2) \right) \quad \text{for } r_i - S/2 \leq r \leq r_i$$

Similarly, excess pore pressure u in Zone B ($r_i \leq r \leq r_i + S/2$) is determined by:

$$[7] \quad u_B = \frac{\gamma_w}{2k_h} \frac{\partial \varepsilon}{\partial t} \left((r_i + S/2)^2 \ln \left(\frac{r}{r_i} \right) - \frac{1}{2} (r^2 - r_i^2) \right) \quad \text{for } r_i \leq r \leq r_i + S/2$$

It is noted that subscripts *A* and *B* are denoted for Zones A and B, respectively and subscript ‘ring’ is denoted for circular loading.

The average excess pore pressure (\bar{u}) is determined from:

$$[8] \quad \bar{u}_{ring} \pi \left((r_i + S/2)^2 - (r_i - S/2)^2 \right) l = \int_0^l \int_{r_i - S/2}^{r_i} 2\pi \mu_A r dr dz + \int_0^l \int_{r_i}^{r_i + S/2} 2\pi \mu_B r dr dz$$

Integrating Equation (8) after substituting Equations (6) and (7), the average excess pore pressure is given by:

$$[9] \quad \bar{u}_{ring} = \frac{\gamma_w}{k_h} \frac{\partial \varepsilon}{\partial t} \frac{1}{8} d_e^2 \mu_{ring}$$

where,

$$[9a] \quad \mu_{ring} = \frac{\alpha^2}{i} \left[\begin{aligned} &2(i - 0.5)^4 \ln \frac{i}{i - 0.5} + \frac{1}{4} (2i - 0.5) (-2i^2 + 3i - 0.75) + \\ &2(i + 0.5)^4 \ln \left(\frac{i + 0.5}{i} \right) - \frac{1}{4} (2i + 0.5) (2i^2 + 3i + 0.75) \end{aligned} \right]$$

$$\approx \frac{2\alpha^2}{3}$$

$$[9b] \quad S = \alpha d_e$$

$\alpha=0.887$ and 0.952 for drains installed in a square pattern and an equilateral triangular pattern, respectively (Holtz et al. 1991).

It is of interest to note that the value of μ_{ring} converges to $\frac{2\alpha^2}{3}$ for all values of ($i > 1$) (Table 2).

Combining Equation (9) with the well-known compressibility relationship

($\partial\varepsilon/\partial t = -m_v \partial\bar{u}/\partial t$) yields:

$$[10] \quad \bar{u}_{ring} = -\frac{\gamma_w}{k_h} m_v \frac{\partial\bar{u}}{\partial t} \frac{1}{8} d_e^2 \mu_{ring}$$

Rearranging the above Equation (10) and then integrating by applying the initial boundary condition $\bar{u} = \sigma_1$ at $t=0$ gives:

$$[11] \quad \frac{\bar{u}_{ring}}{\sigma_1} = \exp\left(\frac{-8T_{h,ring}}{\mu_{ring}}\right)$$

$$[12] \quad U_{h,ring} = 1 - \exp\left(\frac{-8T_{h,ring}}{\mu_{ring}}\right)$$

Equivalent Parameters for Multi-drain Analysis under 2D Axisymmetric Condition

Equivalent parameters can be determined either by geometric transformation or permeability transformation or both to minimise the disparity between the two methods (Indraratna and Redana 2000). For circular loading, the proposed ‘conversion’ procedures can be based on the equivalent average excess pore pressure by maintaining the geometric equivalence (see Fig. 3).

At a given stress level and at each time step, the average excess pore pressure for both the unit cell and a unit of i^{th} revolving prism of soil ($i>1$) are made the same by equating Equation (1) with Equation (12). The equivalent permeability for the multi-drain under axisymmetric condition can then be expressed as:

$$[13] \quad \frac{k_{h,ring}}{k_h} = \frac{\frac{2}{3}\alpha^2}{\left[\ln\left(\frac{n}{s}\right) + \frac{k_h}{k_s} \ln(s) - \frac{3}{4} \right]}$$

MODEL VALIDATION

Finite element program ABAQUS (Hibbitt et al. 2006) based on Biot's consolidation theory was used with assumed soil properties to validate the proposed analytical solution. An elastic analysis was conducted with $m_v=10^{-3}$ m²/kN and simulating the condition of no lateral strain ($v=0$) for validating the proposed solution (Eqn. 11). A total of 3200 axisymmetric elements (8-node bi-quadratic displacement and bilinear pore pressure) were used in the finite element model to simulate a 10m long vertical drain with a spacing of 1.5m (Figures 4a and 4b). A c_h value of 0.32 m²/yr and d_e of 1.575 m (i.e. equivalent to $S=1.5$ m for triangular drain pattern) were used. The aspect ratio of the finite elements was kept below 3. The horizontal undisturbed soil permeability (k_h) was taken as 10^{-10} m/s, and the ratio of the undisturbed permeability to the smear zone permeability (k_h/k_s) and the value of (d_s/d_w) ratio were assumed to be 4.0 and 2.0, respectively. The top, bottom and outer boundaries were set as impermeable (see Figure 4b). The vertical loading pressure ($\sigma_1=50$ kPa) was applied at the top of the cell, and only vertical displacement was allowed. Rigid elements were selected at the soil surface to ensure the equal strain condition.

Figure 5 shows the comparison between the analytical and numerical models before and after conversion for $i=2$ and 15. It can be seen from Equation 11 that the degree of consolidation of a particular soil-drain wall does not depend on the value of i , hence, for the purpose of clarity, the numerical results for $i=2$ and 15 are compared separately in Figures 5a and 5b. Before incorporating the equivalent soil permeability from Equation (11), a good agreement between the numerical and analytical results was obtained by Equation (13). Small deviations are noted for the range $300 < t < 1000$ days with a maximum error of about 5% in the degree of consolidation. It can be seen after incorporating Equation (13) in the numerical model, that the consolidation response agrees with Equation 1. In general, the above matching procedure

confirms the reliability of the proposed procedure after transforming the true field condition to the equivalent axisymmetric drain rings.

APPLICATION TO CASE HISTORY

In 1957, the Swedish Geotechnical Institute and the Swedish Road Broad designed and constructed four circular test embankments to study consolidation behaviour of the soft clay and to obtain information for construction of a new airport (Hansbo, 1960). The site is located on an island about 25 km west of Stockholm, Sweden. Sand drains were installed at three of these test embankments. This study deals with circular test embankment (area II) which was constructed between June and July 1957, with a base diameter of 35 m, slope of 1.5H:1V and height of 1.5 m. Gravel of unit weight of 17.9 kN/m^3 was used as the embankment surcharge after removing 0.25m of the top soil. Sand drains of 0.18m diameter were installed in a triangular pattern at a spacing of 1.5 m. The water table was located 1.0m below the ground surface. The settlement plates, piezometers and horizontal settlement gauges were installed to measure the vertical displacement, pore water pressure and lateral displacements, respectively. The locations of the instrumentations were shown earlier in Fig. 1.

Site Geology and Geotechnical properties:

The site geology and geotechnical properties of soil were described in details by Hansbo (1960) and have been presented in several publications (Holtz and Broms, 1972 and Hansbo, 2005). Only a summary is given here. The geologic stratification of the site area can be described as composed of very recent glacial and postglacial clay deposits. The ground surface is about 2.5 m above the mean level of the Baltic Sea. The deepest sediments consist of glacial clays, which are about 7500 years old while the upper postglacial soils were

deposited within the past 4500 years. In general, these deposits can be described as soft, normally consolidated clay of moderate sensitivity. Site investigations showed that the subsoil conditions are relatively uniform throughout the site, consisting of a weathered crust formed by cyclic wetting process together with natural cementation with a total thickness of 1 m, overlying the soft clay layer extending to about 8-10m below the surface, followed by bedrock or very dense glacial deposits at a depth of 10 to 12 m. The groundwater table is about 1m below the ground surface. The bulk unit weight generally increased from 15 kN/m³ near the ground surface to 17 kN/m³ at the bottom of the soil profile. The compression and consolidation characteristics of the clay were determined using conventional oedometer test. As shown in Fig.1, surface and subsurface settlement plates, hydraulic piezometers, a concrete block and inclinometer were installed to monitor the embankment behaviour. However, due to malfunction of the inclinometer, only the surface lateral displacement measured by the concrete block are available (Holtz and Broms, 1972).

Finite Element Analysis of Circular Embankment

The finite element mesh consisted of 28160 rectangular CAX8RP elements (8-node biquadratic displacement, bilinear pore pressure) as shown in Fig. 6. Only one-half of the embankment was simulated to exploit the symmetry. The relevant soil parameters of 4 subsoil layers are summarised in Table 1 based on the laboratory test results provided by Hansbo (1960). For the topmost over-consolidated crust, the Mohr-Coulomb model was considered appropriate. Based on Hansbo (1997), it was assumed that the diameter of the smear zone (d_s) was 0.36m and that both the permeability of the smear zone (k_s) and the vertical soil permeability (k_v) are 0.25 times the horizontal undisturbed soil permeability (k_h). The well resistance is neglected in the analysis due to sufficient drainage capacity of the drains > 150m³/ year. For the multi-drain analysis, the permeability of soil for each layer

under the circular embankment loading was calculated based on Equation (13). Embankment surcharge loading of 27 kPa was simulated by applying linearly incremental vertical loads to the upper boundary for 30 days, followed by the rest period.

Discussions of the Results

In this section, the predictions based on the multi-drain analysis under both axisymmetric and plane strain conditions are compared with the field measurements. Equation (13) was incorporated in the axisymmetric condition, whereas the equivalent plane strain approach proposed by Indraratna and Redana (2000) was adopted for the plane strain condition. Figures 7a and 7b show the comparison between the predicted and recorded field settlements, (a) at the centreline of the embankment at the ground surface, (b) at a depth of 5m and (c) at a depth of 1.5m and 7m away from the embankment centreline. It can be seen that the predicted settlements from the axisymmetric conditions using Equation (13) agree with the measured results as well as with those predicted by Hansbo (1997), whereas the plane strain analysis underpredicts the field results but gives the same ultimate settlement. Undoubtedly, the excess pore pressure predictions from both cases at 5m depth and at a lateral distance of 0.75m away from the embankment centreline also agree with the field measurements (Fig. 8a). However, the predicted excess pore pressures from the plane strain analysis dissipate faster than that under axisymmetric condition (Fig. 8b). Figure 9 illustrates the surface settlement profile after 452 days, which shows that plane strain condition gives less settlement at the centreline and more heave at the embankment toe.

The comparisons between the measured and predicted lateral movements at 1.5m from the embankment toe are shown in Fig. 10. The predictions from the axisymmetric condition agree well with the measured results, whereas the plane strain analysis over-predicts the measurements (Fig. 10a). Due to insufficient field data, only the predicted lateral

displacements are compared in Fig. 10b. The maximum lateral displacement is observed at the middle of the soft clay layer at a depth of 6m (Fig. 10b). The lateral displacement profiles at the ground surface are shown in Fig. 11. It is seen that the predictions from the axisymmetric condition are always less than those of the plane strain. In general, for a circular embankment improved by vertical drains, the axisymmetric analysis with an appropriate conversion procedure is essential to obtain accurate predictions, in terms of settlement, excess pore pressure and lateral displacement.

CONCLUSIONS

The paper presented a new technique to model consolidation by vertical drains below a circular loaded area where the system of vertical drains in the field was transformed by a series of equivalent concentric cylindrical drain walls. A rigorous solution for radial drainage towards these equivalent walls was derived by matching the degree of consolidation of Hansbo's unit cell model (Hansbo, 1997). An equivalent value for the coefficient of horizontal permeability could be obtained to analyse the multi-drain problem under circular loading.

A multi-drain analysis based on the proposed conversion was adopted to evaluate the performance of a selected full-scale circular embankment at Skå-Edeby, Sweden, using the finite element code, ABAQUS. The effect of smear associated with the sand drains was also considered in the analysis. Unlike unit cell analysis, the settlements, excess pore water pressures and lateral movements elsewhere in the embankment were analysed and compared with the available field data by employing the proposed conversion procedure. Comparisons made with the corresponding predictions using the proposed conversion and Hansbo's solution showed that the predicted results from proposed conversion are more accurate than those from Hansbo's solution apart from the centreline of the embankment. The multi-drain

analysis under equivalent axisymmetric condition using the proposed conversion gives more accurate prediction, whereas the equivalent plane strain FEM analysis tends to underpredict settlements and excess pore pressure by approximately 20%. Moreover, lateral displacement prediction under plane strain condition is almost two times that from the axisymmetric condition. The predictions of soft soil improved by vertical drains under circular loading are more accurate when using multi-drain analysis under equivalent axisymmetric condition.

ACKNOWLEDGEMENT

The second Author gratefully acknowledges the financial support under Endeavour program, Department of Educational, Science and Training, Australia.

REFERENCES

- Barron, R.A. 1948. Consolidation of fine-grained soils by drain wells. Transactions ASCE, **113**: 718-754.
- Chai, J.C., Shen, S.L., Miura, N. and Bergado, D.T. 2001. Simple method of modelling PVD improved subsoil. J. of Geotechnical Engineering, ASCE, **127**(11): 965-972.
- Hansbo, S. 1960. Consolidation of clay with special reference to influence of vertical sand drains. Swedish Geotechnical Institute, Proc., No. 18, 160 p.
- Hansbo, S. 1981. Consolidation of fine-grained soils by prefabricated drains. *In* Proceedings of 10th International Conference on Soil Mechanics and Foundation Engineering, Stockholm, Balkema, Rotterdam, **3**, pp. 677-682.
- Hansbo, S. 1997. Aspects of vertical drain design: Darcian or non-Darcian flow. Geotechnique, **47**(5): 983-992.
- Hansbo, S. 2005 .Experience of consolidation process from test areas with and without vertical drains. In: B. Indraratna and J. Chu (Eds), Ground Improvement—Case Histories, Elsevier, Amsterdam, pp. 3–50.
- Hibbitt, Karlsson, and Sorensen 2006. ABAQUS/Standard User's Manual, Published by HKS Inc.
- Hird, C.C., Pyrah, I.C. and Russell, D. 1992. Finite element modelling of vertical drains beneath embankments on soft ground. Geotechnique, **42**(3): 499-511.
- Holtz, R. D. and Broms, B. 1972. Long-term loading tests at Ska-Edeby, Sweden. Proceedings ASCE specialty conference on performance of earth and earth-supported structures, Purdue University, **1**, pp. 435–464.

- Holtz R.D., Jamiolkowski M.B., Lancellotta R., and Pedroni R. 1991. Prefabricated Vertical Drains: Design and Performance. CIRIA: London; 1-131.
- Indraratna B., and Redana I.W. 2000. Numerical modelling of vertical drains with smear and well resistance installed in soft clay. *Canadian Geotechnical Journal*, **37**(1):133-145.
- Indraratna, B., Balasubramaniam, A. S. and Balachandran, S. 1992. Performance of test embankment constructed to failure on soft marine clay. *J. Geotech. Eng., ASCE*, No. 118, pp. 12-33.
- Indraratna, B., Rujikiatkamjorn C., and Sathananthan, I. 2005. Analytical and numerical solutions for a single vertical drain including the effects of vacuum preloading. *Canadian Geotechnical Journal*, **42**: 994-1014.
- Jamiolkowski, M., Lancellotta, R., and Wolski, W. 1983. Pre-compression and speeding up consolidation. *In Proceedings of 8th European Conference on Soil Mechanics and Foundations*, Helsinki, Finland, **3**, pp.1201-1206.
- Olson, R.E. 1998. Settlement of embankments on soft clays. *Journal of Geotechnical and Geoenvironmental Engineering*, ASCE, **124**(4): 278–288.
- Rixner, J.J., Kraener, S.R., and Smith, A.D. 1986. Prefabricated vertical drains. Summary of research effort-final report. Federal Highway Administration, Report FHWA-RD-86-169, U.S. Department of Commerce, Washington D.C, Vol. 2.
- Yoshikuni, H., and Nakanodo, H. 1974. Consolidation of Fine-Grained Soils by Drain Wells with Finite Permeability. *Japan Soc. Soil Mech. and Found. Eng.* **14**(2): 35-46.

List of Table

Table 1. Soil Properties Used in the Analysis (Hansbo 1960)

Table 2. Relationship of i and μ_{ring} / α^2

List of Figures

Figure 1 Embankment vertical cross section and locations of instrumentation at Skå-Edeby, Sweden (Hansbo 1960)

Figure 2. Conversion for multi-drain system under circular loading adopted for analytical solutions (a) Actual field condition and (b) Equivalent axisymmetric condition

Figure 3 (a) Multi-drain system under axisymmetric condition (b) a single hollow cylinder of soil-drain

Figure 4 (a) Nodes and integration points for a single 8-node bi-quadratic displacement, bilinear pore pressure axisymmetric element (b) Mesh discretization for a single hollow cylinder of soil-drain (not to scale)

Figure 5 Comparison of analytical model with the equivalent model before and after conversion (a) $i=2$, (b) $i=15$.

Figure 6. Finite element mesh

Figure 7. Settlements (a) Surface at the centreline (b) 5m depth at the centreline and (c) 1.5m depth at 7m away from the centreline

Figure 8. Excess pore pressure (a) at 5m depth and 0.75m from the centreline and (b) at 5m depth and 10m away from the centreline

Figure 9. Surface settlement profile after 452 days

Figure 10. (a) Lateral displacements at the surface at 1.5 m from the embankment edge (b) Lateral displacement profile at 1.5m from the embankment edge after 300 days

Figure 11. Lateral displacement profiles at surface after 250 days

Table 1. Soil Properties Used in the Analysis (Hansbo 1960)

	Layer 1	Layer 2	Layer3	Layer 4
Depth (m)	0.00- 1.00	1.00-3.00	3.00-6.00	6.00-11.00
Unit Weight (kN/ m ³)	14.2	14.5	15.6	16
Pre-consolidation Pressure(kPa)	27	24	35	48
k_v and k_s (m/year)	0.0075	0.0064	0.005	0.008
k_h (m/year)	0.03	0.026	0.02	0.032
k_{hring} (m/year) (Eq. 13)	0.00289	0.002505	0.001927	0.003083
λ		0.93	1.55	1.54
κ		0.093	0.155	0.154
Undrained Shear Strength (kPa)		12	8	10
c' (kPa)	30			
ϕ'	30			
E (MPa)	2.7			

Table 2. Relationship of i and μ_{ring} / α^2

i	μ_{ring} / α^2
1	0.691978
2	0.672935
3	0.669448
4	0.668230
5	0.667667
6	0.667361
7	0.667177
8	0.667057
9	0.666975
10	0.666917
11	0.666873
12	0.666840
13	0.666815
14	0.666794
15	0.666778
16	0.666764
17	0.666753
18	0.666744
19	0.666736
20	0.666729

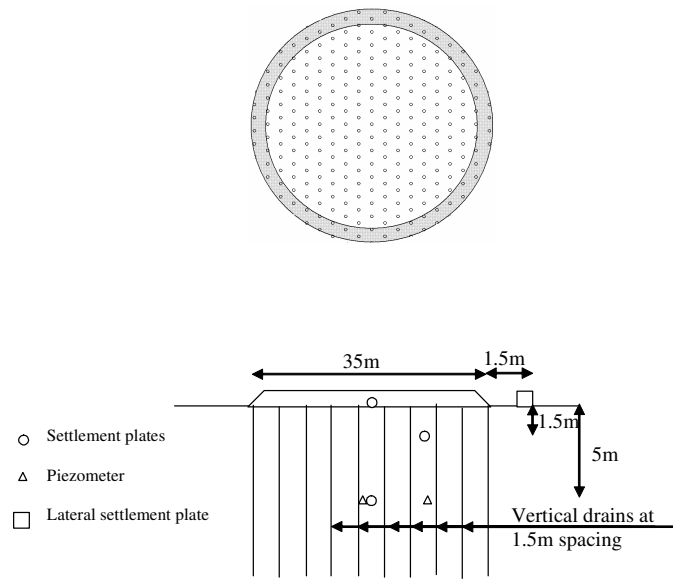


Figure 1 Embankment vertical cross section and locations of instrumentation at Skå-Edeby, Sweden (Hansbo 1960)

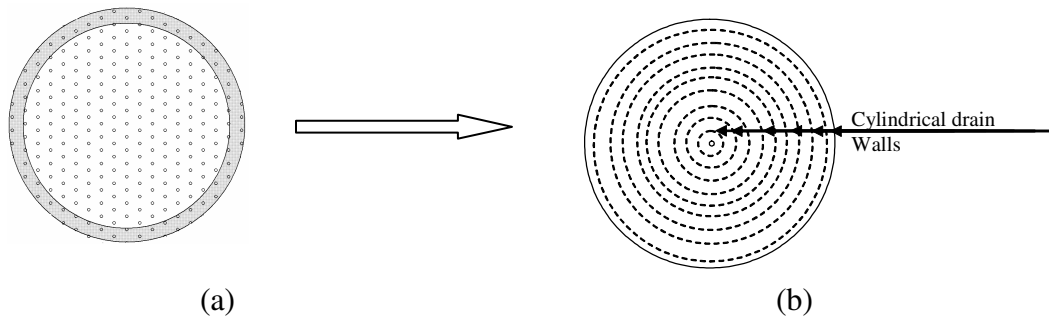
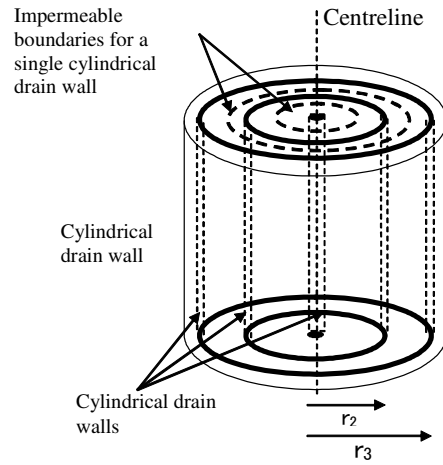
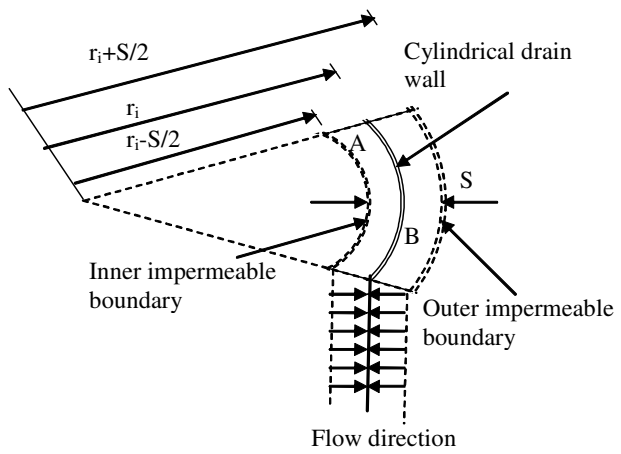


Figure 2. Conversion for multi-drain system under circular loading adopted for analytical solutions (a) Actual field condition and (b) Equivalent axisymmetric condition

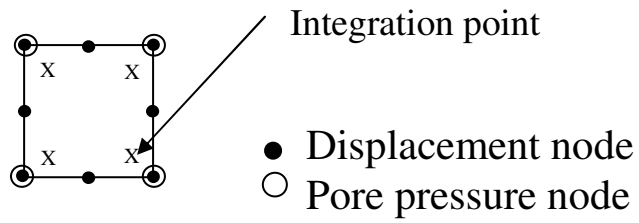


(a)

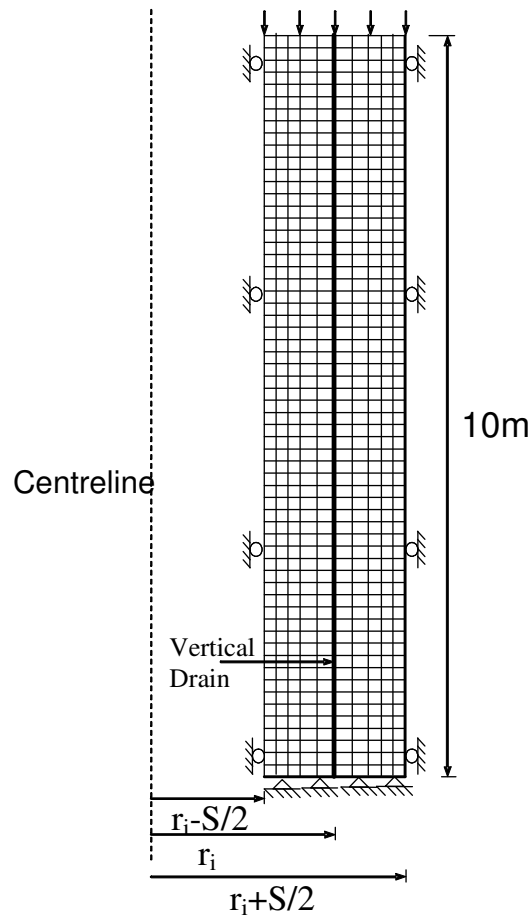


(b)

Figure 3 (a) Multi-drain system under axisymmetric condition (b) a single hollow cylinder of soil-drain

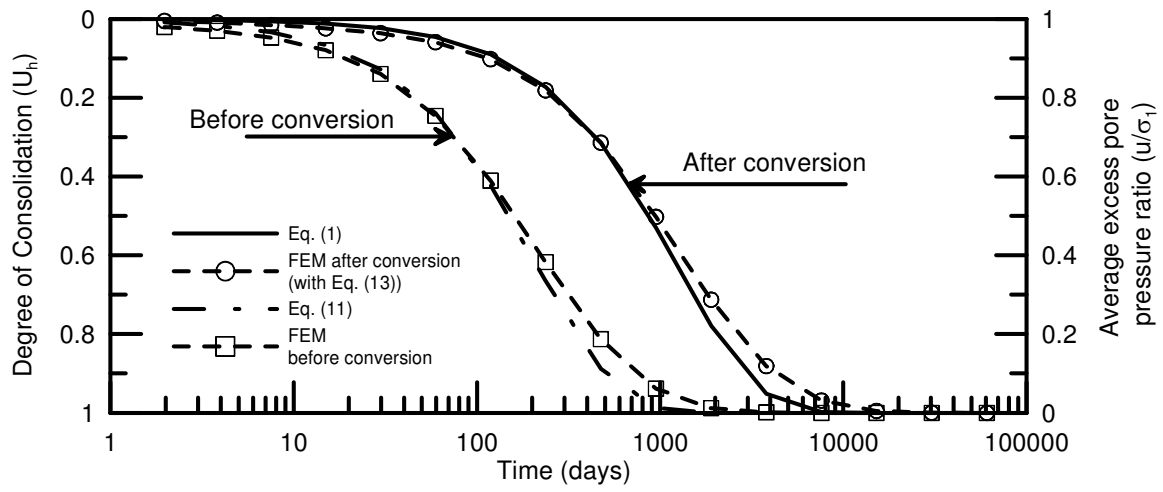


(a)

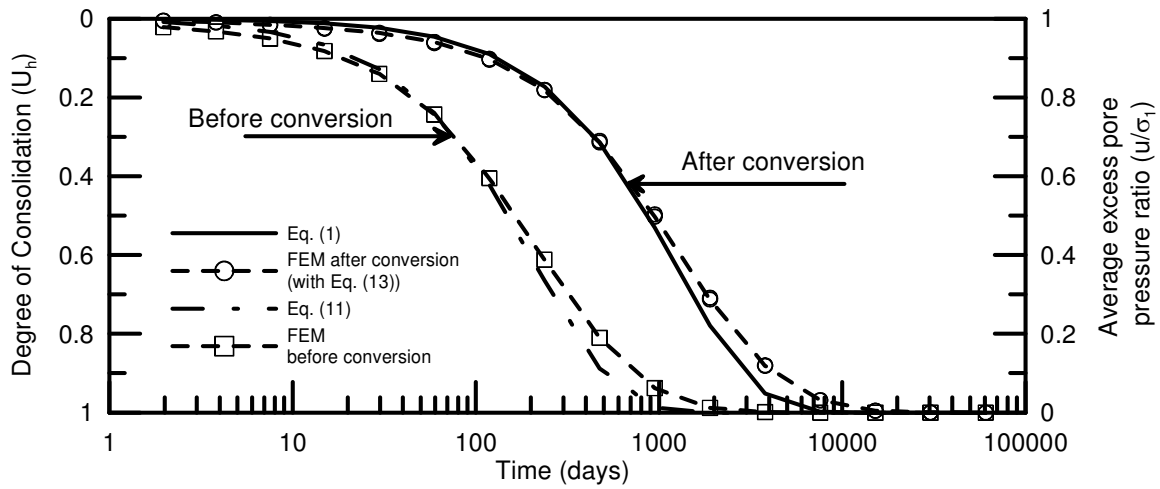


(b)

Figure 4 (a) Nodes and integration points for a single 8-node bi-quadratic displacement, bilinear pore pressure axisymmetric element (b) Mesh discretization for a single hollow cylinder of soil-drain (not to scale)



(a)



(b)

Figure 5 Comparison of analytical model with the equivalent model before and after conversion (a) $i=2$, (b) $i=15$.

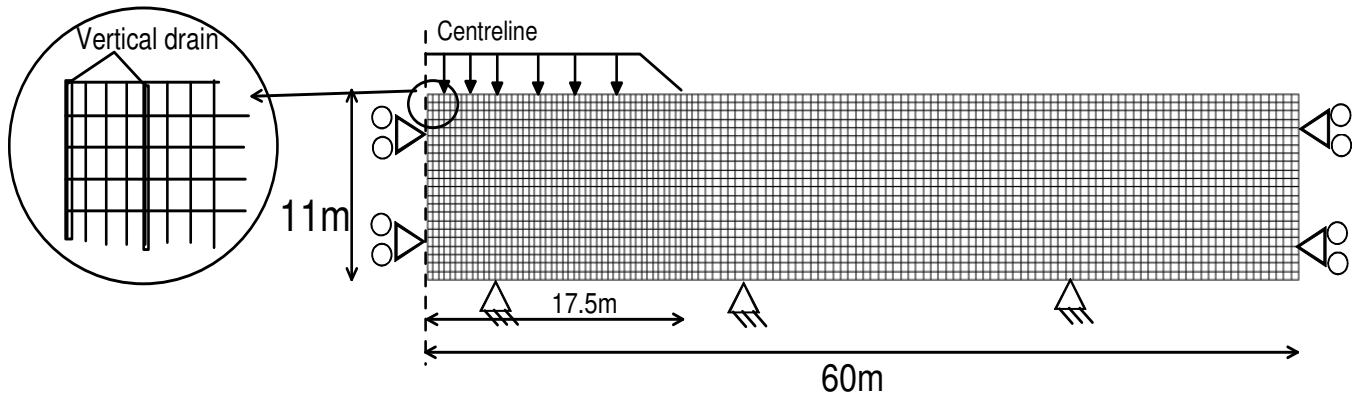
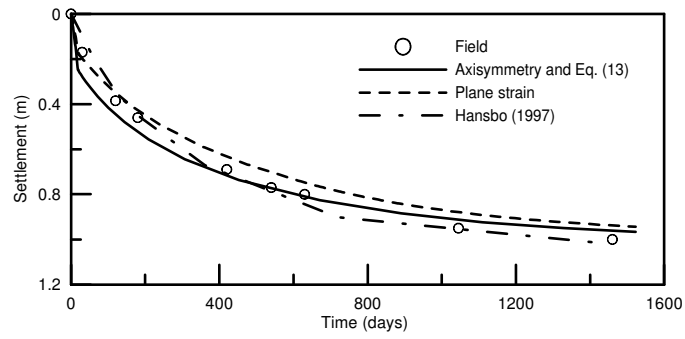
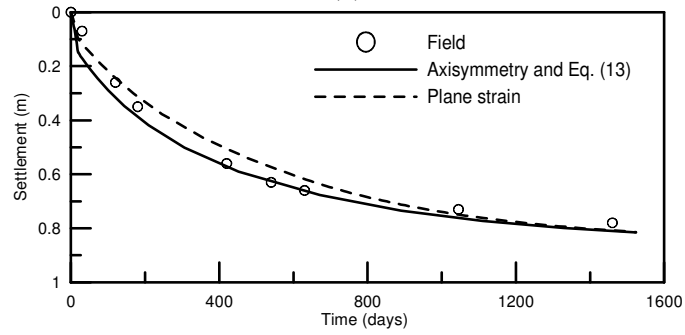


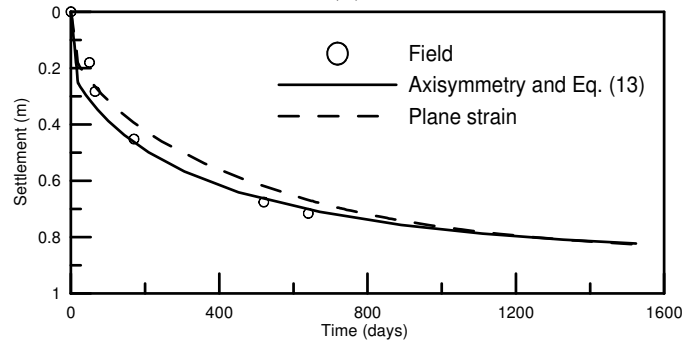
Figure 6. Finite element mesh



(a)

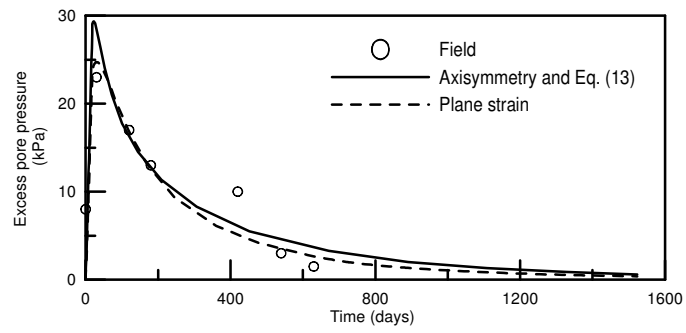


(b)

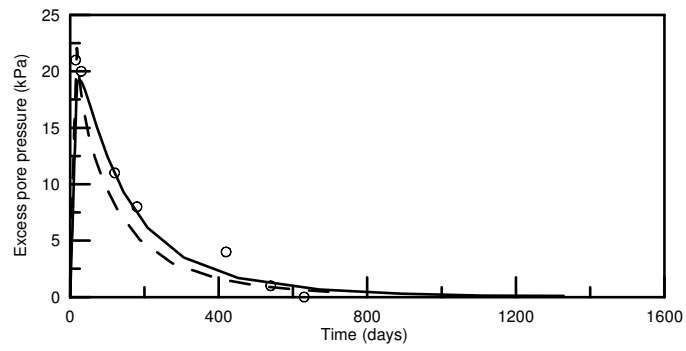


(c)

Figure 7. Settlements (a) Surface at the centreline (b) 5m depth at the centreline and (c) 1.5m depth at 7m away from the centreline



(a)



(b)

Figure 8. Excess pore pressure (a) at 5m depth and 0.75m from the centreline and (b) at 5m depth and 10m away from the centreline

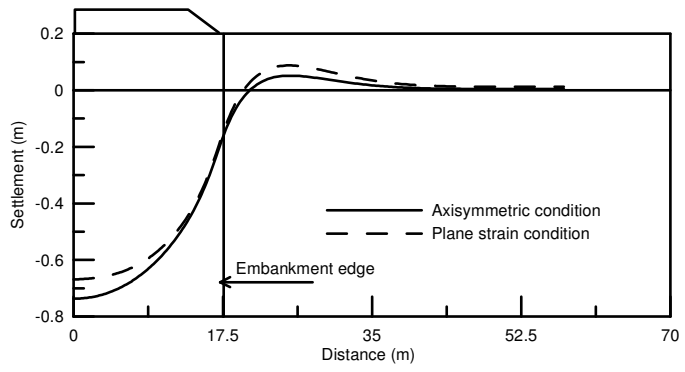
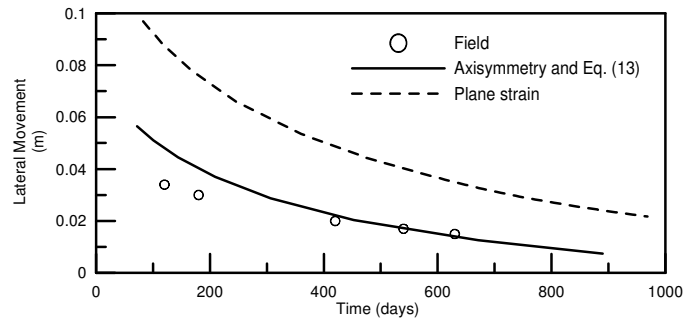
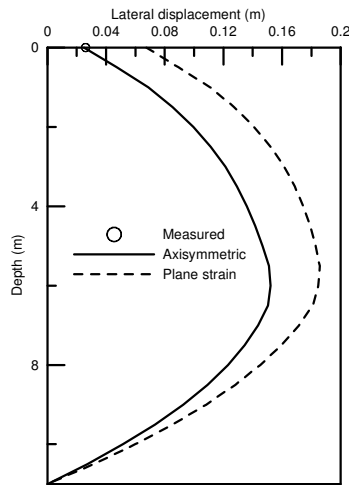


Figure 9. Surface settlement profile after 452 days



(a)



(b)

Figure 10. (a) Lateral displacements at the surface at 1.5 m from the embankment edge (b) Lateral displacement profile at 1.5m from the embankment edge after 300 days

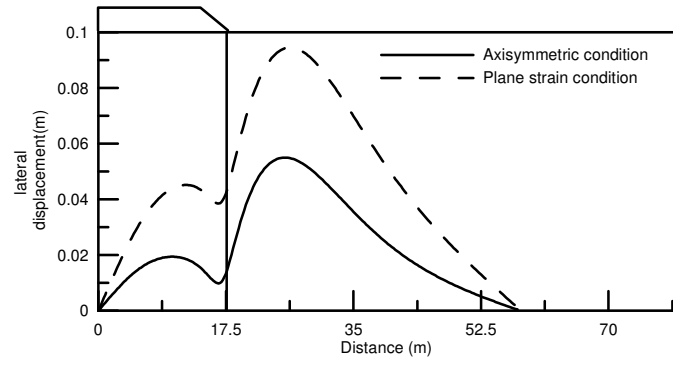


Figure 11. Lateral displacement profiles at surface after 250 days